

Impurity Transport Investigations at W7-AS

BURHENN Rainer*, ANTON Mathias, BALDZUHN Jürgen, BRAKEL Rudolf,
GIANNONE Louis, HACKER Herbert, HIRSCH Mathias, LEDL Ludwig,
MAASSBERG Henning, UNGER Erdmann, WELLER Arthur,
the W7-AS Team, the ECRH Group¹ and the NI Group

Max-Planck-Institut für Plasmaphysik, EURATOM Ass., D-85748 Garching, Germany

¹*Institut für Plasmaforschung, Universität Stuttgart, D-70569 Stuttgart, Germany*

(Received: 30 September 1997/Accepted: 22 October 1997)

Abstract

In order to study the density dependence of impurity confinement in ECF-heated W7-AS plasmas, impurity transport coefficients were derived from SX-camera radiation during aluminum injection by laser blow-off at two different electron densities ($n_{eo} = 3.5/7 \times 10^{19} \text{ m}^{-3}$). At high density, the diffusion coefficient turned out to be smaller by a factor of 2-3. This result is qualitatively compatible with the temporal increase of intrinsic impurity radiation during high density discharges due to reduced transport. The helium concentration did not show a temporal evolution in both cases. No striking differences in MHD-activity, radial electric field or density fluctuations were observed.

Keywords:

stellarator, W7-AS, impurity transport, laser blow-off

1. Introduction

For the decay time of injected tracer impurities (aluminum laser blow-off) in W7-AS, the electron density is, among others, an important scaling parameter [1], indicating improved confinement of impurities towards high electron density. This observation could not simply be attributed to a decrease in Z_{eff} . Similar dependence of impurity confinement within a certain density range was already observed in ECF heated Heliotron E plasmas [2], where the change in transport was supposed to be caused by changes in the diffusion coefficient D rather than in the flow velocity v , the latter being close to classical expectations. Previous impurity injection experiments at W7-AS (H_2S gas oscillation and Al laser blow-off) [1] at medium density ($n_{eo} = 2-5 \times 10^{19} \text{ m}^{-3}$) could partially be simulated within the errors by the one-dimensional radiation and transport code SITAR [3], based on neoclassical and Pfirsch-Schlüter transport for axisymmetric devices. At low

density, the transport was found to be significantly higher than predicted, whereas at high density ($n_{eo} = 6.5 \times 10^{19} \text{ m}^{-3}$), the neoclassical fluxes had to be reduced to fit the experimental data. In order to elucidate this density dependence, discharges with densities varied by a factor of 2 ($n_{eo} = 3.5/7 \times 10^{19} \text{ m}^{-3}$) were analyzed in more detail, together with fluctuation- and MHD-diagnostics and measurement of the radial electric field. Especially in non-axisymmetric devices like stellarators, the latter can play an important role for impurity transport [4], but is not yet included in SITAR.

Simulations with simple assumptions about $D(r)$ - and $v(r)$ -profiles might mask possible local changes in transport. Therefore, the radial transport coefficients were tried to be directly derived from the temporal and radial behaviour of integrated spectral radiation, detected by the SX-camera during the penetration process of injected aluminum by laser blow-off. Indications

*Corresponding author's e-mail: burhenn@ipp.mpg.de

about the radial location of the transport modification at different densities were expected.

2. Transport Analysis

Because of its good radial and temporal resolution, the SX-camera is a proper diagnostic tool at W7-AS for transport investigation. In the case of tracer injection, the pure contribution of tracer radiation was obtained by subtraction of a discharge without injection. In spite of its energy-integrated information, the use of a $25\text{ }\mu\text{m}$ Be-filter in front of the camera offers the possibility to restrict the number of ionization states contributing to the measured intensity and simplifies the reconstruction of the total tracer density profiles. For total aluminum density reconstruction during the penetration process of injected aluminum, the radial intensity profile at each time-step was Abel-inverted (Fig. 1b): injection time $t = 0.5\text{ s}$ and converted to a total aluminum density profile assuming coronal equilibrium (quasi-stationary condition) in a first step. This is considered to be applicable

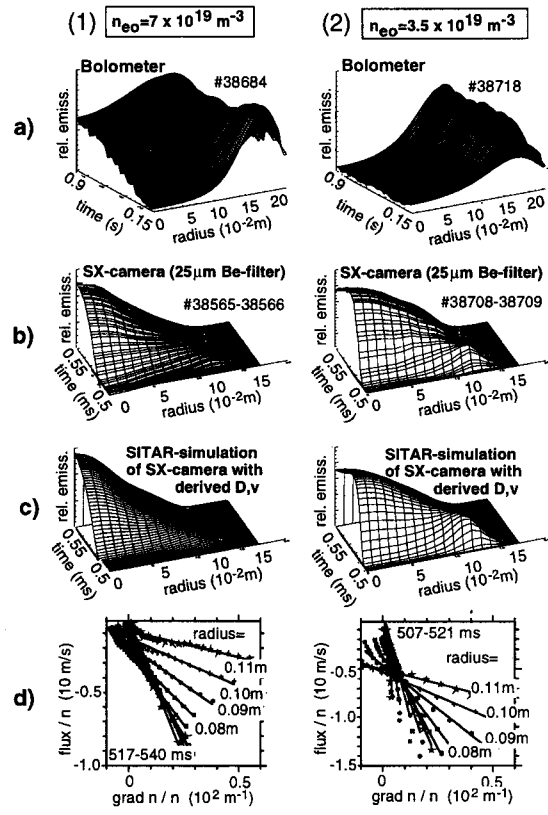


Fig. 1 Evolution of radiation at medium and high density:
(a) total radiation, (b) SX-camera radiation during impurity injection, (c) simulation of SX-radiation with derived D, v , (d) graphical derivation of D, v from aluminium density profile evolution.

in low-transport discharges at high electron density. The transport coefficients at a certain radial position can then be derived from the local temporal evolution of the total aluminum density profiles $n(r, t)$ [5]. With the ansatz $\Gamma = -D \operatorname{grad}(n) + vn$, D and v can be determined by fitting a straight line, when plotting the normalized total aluminum fluxes Γ/n vs. the normalized total aluminum density gradients $\operatorname{grad}(n)/n$ for all times at this radial position (Fig. 1d)). The flux Γ can be estimated from the density profile evolution using the continuity equation $\operatorname{dn}/\operatorname{dt} = -\operatorname{div}(\Gamma)$ with restriction to radial regions where external sources and sinks can be neglected.

In cases where the assumption of quasi-stationarity might not hold, the reconstruction with coronal equilibrium can cause errors. Therefore, the radial density profiles for each time step were reconstructed again, now using a reconstruction factor $\beta(r, t) = n(r, t)/P(r, t)$ (P : total local emissivity contributing to SX-camera) obtained from a transport and radiation calculation with SITAR, using the D - and v -values derived in the first step as input. A repeated derivation procedure for D and v , but now with the corrected density profile evolution as described above, provides new transport coefficients (Fig. 2) which, in fact, fit the SX-camera better in most cases (Fig. 1b, c)). The accuracy of this iterative method strongly relies on the quality of Abel-inversion and atomic data base. Bremsstrahlung and

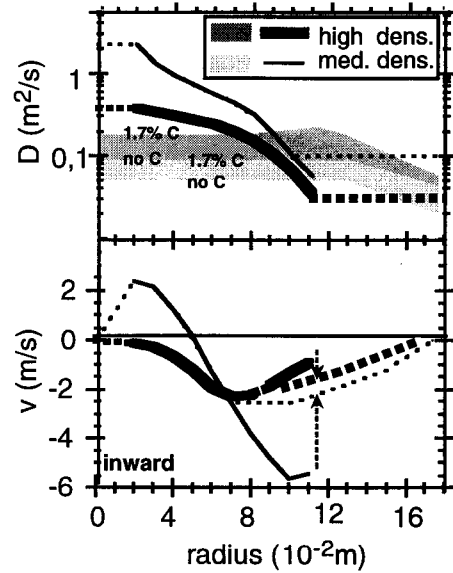


Fig. 2 Derived transport coefficients D, v at medium (thin curve) and high (thick curve) electron density (dotted lines: extrapolations, arrows: corrections, shaded areas: predictions by SITAR).

radiation from dielectronic recombination and inner-shell processes were not yet implemented in SITAR, but were checked to contribute not more than 20% to the SX-radiation in the case of stationary conditions. Possible errors have to be discussed in this context.

3. Results and Discussion

In order to study the density dependence of impurity confinement at W7-AS, ECF-heated discharges ($P_{\text{ECF}} = 480 \text{ kW}$, $\iota = 0.338$, $B = 2.56 \text{ T}$, $a = 0.173 \text{ m}$) at two different densities ($n_{\text{eo}} = 3.5/7 \times 10^{19} \text{ m}^{-3}$) were compared. The transport coefficients were derived according to the procedure described above (Fig. 1) and are plotted in Fig. 2 for both densities.

For the outer plasma region, the last reliably determined value of the diffusion coefficients at $r = 0.10\text{--}0.11 \text{ m}$ were kept constant up to the plasma edge. They represent average diffusion coefficients for this region, determining essentially the central time behaviour during the inflow phase. The extrapolated average diffusion coefficient for medium density approaches the neoclassically predicted one (Fig. 2: light shaded area), but falls below the predictions (Fig. 2: dark shaded area) for the high density case (fluxes in SITAR are already reduced by 50% to account for the W7-AS transport optimization; 1.7% C as additional impurity background concentration was assumed in both cases, compatible with Z_{eff} measurements). This trend is even more pronounced at higher electron densities of $n_{\text{eo}} = 1.2 \times 10^{20} \text{ m}^{-3}$, e.g. in high confinement neutral-beam heated discharges [6], where transport coefficients were derived ($D(r) = 0.07 \text{ m}^2/\text{s}$, $v(r) = 5 \text{ m/s} \cdot (r/a)$, #38551), being clearly smaller than predicted by SITAR.

The convection velocity was extrapolated to vanish in the plasma center and had to be adjusted in the outer part to fit better the temporal decay of spectral line intensities from different ionization states of aluminum, observed by central-line-of-sight crystal- and VUV-spectrometers (Fig. 3: left). For the high density discharge, only a slight correction in the derived v (Fig. 2: see arrows) was necessary to excellently fit all experimental data. In the case of medium density, $D(r = 0.10 \text{ m})$ was used for extrapolation and v , however, has to be reduced by a factor of 2 for a good compromise in fitting the experimental data radially as well as temporally. A reduction of D in the outer region down to the value $D(r = 0.11 \text{ m})$ would fit the time traces of the spectrometers only for the case of vanishing convection velocity, but will lead to a misfit of the radial profiles.

In the two ECF-heated discharges under investiga-

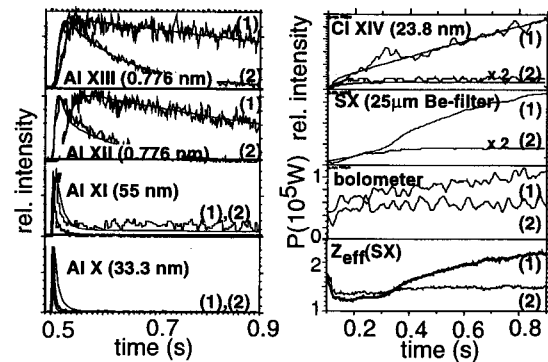


Fig. 3 Left: time traces and simulations of spectral lines from different ionization states of aluminum after injection by laser blow-off: (1) $n_{\text{eo}} = 7 \times 10^{19} \text{ m}^{-3}$, (2) $n_{\text{eo}} = 3.5 \times 10^{19} \text{ m}^{-3}$. Right: time evolution of impurity radiation and $Z_{\text{eff}}(\text{SX})$, and simulations for Cl-XIV.

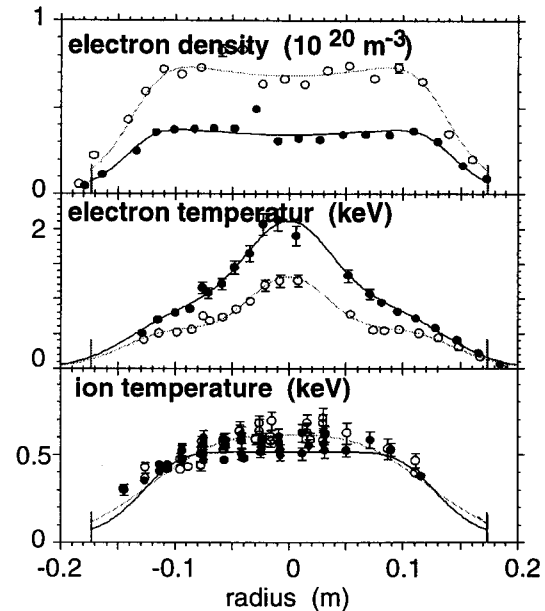


Fig. 4 Electron density, temperature and ion temperature profiles of the investigated ECF-heated discharges: (●) medium, (○) high density.

tion, no clear changes as well in the radial electric field E_r (within the errors) as in MHD-activity, density fluctuation level and radial density and temperature profile shape (Fig. 4) could be observed from which the difference in transport can be deduced reliably.

In the case of high electron density, D is overall lower by a factor of 2-3 compared to the medium density discharge, v being quite similar. The resulting difference in confinement can be illustrated quite impressively by the change in decay time for the injected

aluminium (Fig. 3: left). Consequently, also the time evolution of intrinsic impurity radiation and Z_{eff} is remarkably different during the flat-top phase for this two densities (Fig. 3: right). However, assuming a constant impurity influx of, e.g. intrinsic chlorine from the walls and using just the derived set of transport parameters, the difference in the time traces of Cl-XIV can be qualitatively well described (Fig. 3: see fits): compared to medium electron density, where stationary conditions were achieved well within the pulse length, the reduced transport in the high density case causes longer times to establish stationarity. Similar behaviour for other intrinsic impurity species might explain the signals of SX-camera, bolometer and Z_{eff} (Fig. 3 right, Fig. 1a)). Nevertheless, at high density ($n_{e0} = 7 \times 10^{19} \text{ m}^{-3}$) the extrapolated total radiation (bolometer) at the time when the Cl-XIV radiation should reach 90% of its stationary level (from simulation: approx. at 1.7 s), stays well below the critical value of 60% of the heating power [7], where the plasma is severely affected by radiation. The helium inventory (introduced by a gas-puff and kept in the machine by recycling) as measured by CXRS (He-II at $r = 6 \text{ cm}$) shows no temporal increase in the high density case.

References

- [1] R. Burhenn et al., *Proc. 22nd EPS Conf. on Contr. Fusion and Plasma Physics*, Bournemouth **19C** Part III, 145 (1995).
- [2] H. Kaneko et al., *Nucl. Fusion* **27**, 1075 (1987).
- [3] WVII-A Team and NI Group, *Nucl. Fusion* **25**, 1593 (1985).
- [4] J. Baldzuhn et al., *Proc. 24th EPS Conf. on Contr. Fusion. and Plasma Physics*, Berchtesgaden, **21A** Part IV, 1585 (1997).
- [5] A. Weller et al., *Plasma Phys. and Control. Fusion* **33** 1559 (1991).
- [6] U. Stroth et al., *Proc. 24th EPS Conf. on Contr. Fusion and Plasma Physics*, Berchtesgaden, **21A** Part IV, 1597 (1997).
- [7] P. Grigull et al., *Proc. 24th EPS Conf. on Contr. Fusion and Plasma Physics*, Berchtesgaden **21A** Part IV, 1573 (1997).